

# Analysis and Quantitation of Fructooligosaccharides Using Matrix-Assisted Laser Desorption/Ionization Fourier Transform Ion Cyclotron Resonance Mass Spectrometry

Richard R. Seipert,<sup>†</sup> Mariana Barboza,<sup>†</sup> Milady R. Niñonuevo,<sup>†</sup> Riccardo G. LoCascio,<sup>‡,§</sup> David A. Mills,<sup>‡</sup> Samara L. Freeman,<sup>||</sup> J. Bruce German,<sup>||</sup> and Carlito B. Lebrilla<sup>\*,†,⊥</sup>

Department of Chemistry, Department of Viticulture and Enology, Microbiology Graduate Group, Department of Food Science and Technology, and School of Medicine, University of California, Davis, One Shields Avenue, Davis, California 95616

Inulin is a class of fructooligosaccharide (FOS) derived from plants, which is often used as a natural food ingredient. Inulin is currently used as an additive in baked goods, dairy products, infant formula, and dietary supplements as a result of its purported health-promoting properties. The growth of health-promoting lactobacilli and bifidobacteria is supported by FOS, giving it the classification of a prebiotic; however, its ability to selectively stimulate only beneficial bacteria has not been demonstrated. In order to better understand the role of inulin and FOS as prebiotics, matrix-assisted laser desorption/ionization Fourier transform ion cyclotron resonance mass spectrometry has been used for qualitative and quantitative analysis on bacterial growth. A method using an internal standard has been developed to quantify the consumption of FOS by *Bifidobacterium longum* by *infantis* using a calibration curve. Due to the differential consumption of FOS, the calibration curve was modified to include intensity components for each polymer unit in order to achieve more accurate quantitation. The method described was designed to be more rapid, precise, and robust for quantitative analysis when compared to existing methods.

Oligosaccharides are complex biomolecules that play essential roles in multiple biological processes, including cell–cell recognition, fertilization, immune response, and nutrition.<sup>1–5</sup> Inulin-type

fructooligosaccharides (FOS) are plant-derived oligosaccharides composed of linear fructans with  $\beta$ -(2–1) linkages.<sup>6,7</sup> Inulin has been proposed to act as a beneficial dietary ingredient by acting as a growth-stimulating substrate for bacteria in the human intestine. The potential for such stimulation of bacterial growth to constitute a “prebiotic” effect implies that there is a net improvement in the health of the human host as a direct result of this growth.<sup>8</sup> However, the scientific basis for claims of prebiotic effects remains poorly understood. It is not yet defined which bacteria in the human intestine are actually stimulated, which fractions of inulin are particularly effective, or whether under some circumstances the net effect of inulin on bacterial growth is not beneficial.

The lack of a clear molecule-specific and mechanistic understanding of polysaccharides as bacterial substrates makes it impossible to make strong predictions as to the overall long-term effects of such food ingredients on human health. One of the impediments to building this understanding is the lack of accurate, high-throughput methods to determine the structures and abundances of polymers of FOS and inulin. Previously, inulin and FOS were added to food as an inexpensive way to increase flavor and texture, but as a result of inulin’s, proposed health-promoting properties, it has become a major food supplement and is added to many foods ranging from infant formulas and other dairy products to baked goods and even animal feed. Analytical methods for the analysis of inulin have not advanced as rapidly as its use, and as a result, advanced analytical techniques are needed for the investigation of inulin both qualitatively and quantitatively.

The degree of polymerization (DP) of inulin can range from 2 to 60, depending on the process of preparation and the plant origin.<sup>9</sup> Inulin has been investigated with multiple analytical methods, in order to determine structure, DP, and concentration. These methods include capillary electrophoresis (CE), high-

\* To whom correspondence should be addressed. Telephone: 1-530-752-6364. Fax: 1-530-754-5609. E-mail: cblebrilla@ucdavis.edu.

<sup>†</sup> Department of Chemistry.

<sup>‡</sup> Department of Viticulture and Enology.

<sup>§</sup> Microbiology Graduate Group.

<sup>||</sup> Department of Food Science and Technology.

<sup>⊥</sup> School of Medicine.

- (1) Hakomori, S. *Pure Appl. Chem.* **1991**, *63*, 473–482.
- (2) Cornwall, G. A.; Tulsiani, D. R. P.; Orgebinrist, M. C. *Biol. Reprod.* **1991**, *44*, 913–921.
- (3) Rudd, P. M.; Wormald, M. R.; Dwek, R. A. *Trends Glycosci. Glycotechnol.* **1999**, *11*, 1–21.
- (4) Kunz, C.; Rudloff, S.; Baier, W.; Klein, N.; Strobel, S. *Annu. Rev. Nutr.* **2000**, *20*, 699–722.
- (5) Zhang, X. L. *Curr. Med. Chem.* **2006**, *13*, 1141–1147.

(6) Roberfroid, M. B. *Br. J. Nutr.* **2006**, *93*, S13–S25.

(7) Niñonuevo, M. R.; Park, Y.; Yin, H. F.; Zhang, J. H.; Ward, R. E.; Clowers, B. H.; German, J. B.; Freeman, S. L.; Killeen, K.; Grimm, R.; Lebrilla, C. B. *J. Agric. Food Chem.* **2006**, *54*, 7471–7480.

(8) Gibson, G. R.; Roberfroid, M. B. *J. Nutr.* **1995**, *125*, 1401–1412.

(9) Wang, J.; Sporns, P.; Low, N. H. *J. Agric. Food Chem.* **1999**, *47*, 1549–1557.

performance ion-exchange chromatography with pulsed amperometric detection (HPAEC-PAD), and more recently matrix-assisted laser desorption/ionization (MALDI) time-of-flight (TOF) mass spectrometry (MS).<sup>10,11</sup> While CE and HPAEC-PAD are capable of providing the DP of inulin, primarily through calibration with standards, they do not provide structural information or direct composition. Mass spectrometry can provide both structural information and exact composition. High-performance mass spectrometry can even provide elemental composition with high-mass accuracy determinations. These capabilities are advancing and becoming more available either through time-of-flight or Fourier transform (FT) mass spectrometry, which includes both ion cyclotron resonance (ICR) and orbitrap analyzers. The combination of MALDI and FT-ICR MS provides a sensitive and robust analytical method that also provides high-performance capabilities.<sup>12</sup> They include high-mass accuracy and high resolution that can separate near-isobaric compounds even at high mass for rapid and unambiguous assignments of oligosaccharide signals. FT-ICR MS is also capable of performing multiple methods of tandem MS, which enables the structural elucidation of many complex oligosaccharides.<sup>13</sup> These methods include infrared multiphoton dissociation (IRMPD) and sustained off-resonance irradiation collision-induced dissociation (SORI-CID), which can yield structural information and complementary compositional information.<sup>14</sup>

The intestinal microbiota has been described as an essential "organ". Although this symbiosis is not well understood, several important species of bacteria have been identified and cultured including numerous bifidobacterial species.<sup>15</sup> Different species of bifidobacteria exhibit distinct abilities to ferment complex carbohydrates.<sup>16</sup> Efforts in our laboratory have focused on the development of high-throughput methods for characterizing bacterial consumption of prebiotics. To this end, we describe the use of high-performance mass spectrometry to provide a robust, sensitive, and rapid analytical method that is also quantitative to probe the selective fermentation of FOS by beneficial bacteria.

Until recently, consumption of FOS by *Bifidobacterium longum* was monitored by gas chromatography (GC) by Van der Meulen and co-workers.<sup>17</sup> The use of GC to quantify oligofructose is only applicable to low-mass samples due to the decrease in volatility of the derivatized oligosaccharides at higher mass. Furthermore, due to the time required for sample preparation and analysis, the efficacy of this method for monitoring selective consumption of bacteria is problematic. In order to circumvent some of the problems related to GC, consumption of FOS and inulin have been

investigated with HPAEC-PAD.<sup>18</sup> However, HPAEC-PAD lacks the ability to be high throughput, due to long analysis times and reconditioning of columns. We have recently shown a MS-based method for the selective consumption of human milk oligosaccharides by bifidobacteria employing stable isotope labeling.<sup>19</sup> Similar isotopic labeling is not possible with FOS; consequently, we developed a rapid quantitation method based upon an internal standard that is readily obtainable and possesses chemical properties similar to FOS. This standard was employed to account for spot-to-spot variability that often affects MALDI quantitation in order to quantitate FOS consumption.<sup>20</sup>

## MATERIALS AND METHODS

**Materials and Reagents.** Raftiline high-performance (HP) inulin and Raftilose P95 FOS were provided by Orafit Active Food Ingredients (Malvern, PA). Porous graphitized carbon solid-phase extraction (PGC-SPE) cartridges (150-mg bed mass, 4-mL tube size) for oligosaccharide purification were purchased from Alltech (Deerfield, IL). Sodium borodeuteride (98%), 2,5-dihydroxybenzoic acid (DHB), and maltoheptaose (94%) were purchased from Sigma-Aldrich (St. Louis, MO). Evaporation of solvent was performed using a Labconco Centriva Concentrator (Kansas City, MO). All other reagents were of analytical grade or higher.

**Bacterial Fermentation.** In vitro FOS fermentation experiments were assayed using *B. longum* bv. *infantis* ATCC 15697. Initially cultures were propagated in a MRS medium supplemented with 1% L-cysteine and 1.5% (w/v) lactose as a carbon source.<sup>21</sup> Cultures were then passaged twice in MRS medium supplemented with 1% L-cysteine, containing 1% (w/v) Raftiline P95 as a sole carbon source. Each fermentation experiment was performed in triplicates, and controls consisted of inoculated medium lacking FOS and uninoculated medium containing FOS.

Incubations were carried out at 37 °C in an anaerobic chamber (Coy Laboratory Products, Grass Lake, MI), and cell growth was measured by assessing optical density (OD) at 600 nm with a ND-1000 spectrophotometer (NanoDrop Technologies, Wilmington, DE). Samples were collected at 0, 36, and 60 h postinoculation, centrifuged at 14000g for 10 min, and the resulting supernatant, was boiled in a water for 5 min, filtered with a 0.22- $\mu$ m sterile Millex-GV (Millipore, MA), and stored at -80 °C.

**Oligosaccharide Reduction and Purification.** The maltoheptaose standard (10 mM) was reduced by adding 2.0 M sodium borodeuteride and incubating at 70 °C for 1 h. The fermentation samples and the reduced standard were desalted and purified using PGC-SPE. The cartridges were conditioned with 3 volumes of 80% acetonitrile with 0.1% trifluoroacetic acid (v/v), followed by 3 volumes of deionized water. The oligosaccharide samples were loaded into a PGC-SPE cartridge, washed with 5 volumes of deionized water at a flow rate of 1 mL/min, eluted with 2.5 volumes of 20% acetonitrile/water (v/v), dried in vacuo, and reconstituted in deionized water to initial concentration.

(10) Kazmaier, T.; Roth, S.; Zapp, J.; Harding, M.; Kuhn, R. *Fresenius J. Anal. Chem.* **1998**, *362*, 552–552.

(11) Harvey, D. J. *Mass Spectrom. Rev.* **2006**, *25*, 595–662.

(12) Zhang, L. K.; Rempel, D.; Pramanik, B. N.; Gross, M. L. *Mass Spectrom. Rev.* **2005**, *24*, 286–309.

(13) Zhang, J. H.; Schubothe, K.; Li, B. S.; Russell, S.; Lebrilla, C. B. *Anal. Chem.* **2005**, *77*, 208–214.

(14) Xie, Y. M.; Lebrilla, C. B. *Anal. Chem.* **2003**, *75*, 1590–1598.

(15) Eckburg, P. B.; Bik, E. M.; Bernstein, C. N.; Purdom, E.; Dethlefsen, L.; Sargent, M.; Gill, S. R.; Nelson, K. E.; Relman, D. A. *Science* **2005**, *308*, 1635–1638.

(16) Crociani, F.; Allesandrini, A.; Mucci, M. M. B.; Biavati, B. *Int. J. Food Microbiol.* **1994**, *24*, 199–210.

(17) Van der Meulen, R.; Makras, L.; Verbrugge, K.; Adriany, T.; De Vuyst, L. *Appl. Environ. Microbiol.* **2006**, *72*, 1006–1012.

(18) Rossi, M.; Corradini, C.; Amaretti, A.; Nicolini, M.; Pompei, A.; Zaroni, S.; Matteuzzi, D. *Appl. Environ. Microbiol.* **2005**, *71*, 6150–6158.

(19) Ninonuevo, M. R.; Ward, R. E.; LoCascio, R. G.; German, J. B.; Freeman, S. L.; Barboza, M.; Mills, D. A.; Lebrilla, C. B. *Anal. Biochem.* **2007**, *361*, 15–23.

(20) Luxembourg, S. L.; McDonnell, L. A.; Duursma, M. C.; Guo, X. H.; Heeren, R. M. A. *Anal. Chem.* **2003**, *75*, 2333–2341.

(21) de Man, J. C.; Rogosa, M.; Sharpe, M. E. *J. Appl. Bacteriol.* **1960**, *23*, 130–135.

**MALDI FT-ICR MS Analysis.** All mass analyses were performed with a ProMALDI-FT-ICR MS instrument with an external MALDI source, a 355-nm pulsed Nd:YAG laser, a hexapole accumulation cell, a quadrupole ion guide, and a 7.0-T superconducting magnet (Varian/IonSpec, Lake Forest, CA). The instrument was modified with the addition of a CO<sub>2</sub> laser (10.6 μm, 20-W maximum power, Parallax, Waltham, MA) in order to provide IR photons for the IRMPD experiments.<sup>13,14</sup> The matrix, 1.0 μL of 0.4 M DHB plus 10 μM NaCl, was spotted followed by the addition of 1.0 μL of analyte onto a 100-well stainless steel sample plate (Applied Biosystems, Foster City, CA) according to the fast evaporation method.<sup>22</sup> Each sample was analyzed in the positive ion mode, with external accumulation of ions in the hexapole; collisional cooling of ions was achieved by pulsing in nitrogen at a foreline pressure of 100 Torr during ion accumulation. Ions were then transferred to the ICR cell via the ion guide for excitation and detection. Tandem mass spectrometry of desired precursor ions was performed by isolation of the precursor in the ICR cell via selective ejection. Isolated precursor ions were then irradiated with photons for 500 ms for IRMPD or subjected to SORI amplitudes of 8 V<sub>(b-p)</sub> with a 1000-Hz frequency offset while the ICR cell pressure was raised to 10<sup>-6</sup> Torr via pulsed nitrogen gas.

**Quantitation.** Two different calibration curves were constructed for distinct applications. For quantitation of FOS in foods or for any application in which the composition of FOS does not change, a simple calibration curve was created by plotting the ratio of the DP 7 inulin peak height divided by the deuterated and reduced maltoheptaose standard versus the concentration of FOS. For the cases in which the individual components of the polymer varied in intensity, it was essential to include each DP separately in a weighted fashion (eq 1). In this equation  $R_w$  is the

$$R_w = \sum_i i(I_i/I_s) \quad (1)$$

weighted ratio, which is plotted versus the concentration of FOS,  $i$  is the DP,  $I_i$  is the intensity of the respective DP mass spectral peak, and  $I_s$  is the intensity of the standard peak. Multiple mass spectra were acquired for each point on the calibration curves and averaged; linear least-squares fitting was applied in order to determine the slope and  $y$  intercept. The standard deviation of the slope was calculated, and the  $R^2$  value was used to evaluate the fit. The limit of detection (LOD) was calculated based upon the standard deviation of the intercept and the slope of the line of best fit.

## RESULTS AND DISCUSSION

**Structural Analysis via FT-ICR MS.** Inulin-type fructans are linear carbohydrates composed of β(2–1) fructosylfructose linkages.<sup>6</sup> The terminal position of the carbohydrate either contains glucose or a fructose in the pyranose form while the fructan chain is in the furanose form. Both glucose and fructose monomers have an exact residue mass of 162.0528 Da. The DP varies from 2 to 60 units depending on plant source.<sup>23</sup> The two inulin samples analyzed were composed of inulin extracted from chicory, inulin

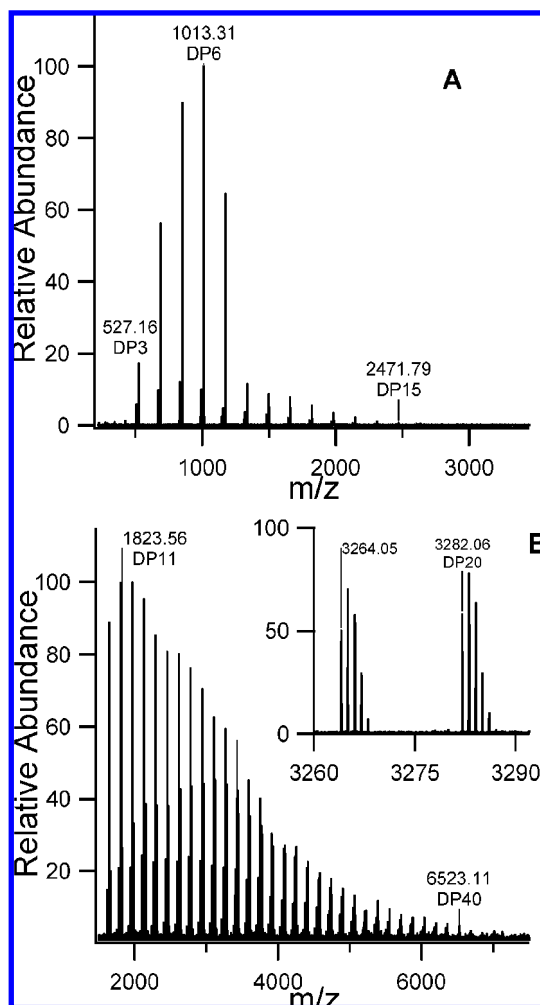


**Figure 1.** MALDI FT-ICR MS positive ion spectra: (A) FOS P95 and (B) inulin HP. These spectra show the DP range for each type of inulin. The inset shows the two major polymeric series: one isotopic envelope corresponds to the intact inulin DP 20, while the other most likely represents a B-type a fragment derived from a larger molecular ion (i.e., DP > 20).

HP being the high-mass fraction, while inulin P95 is a low-mass inulin product from enzymatic hydrolysis of the native inulin using an endoinulinase (EC 3.2.1.7).<sup>6</sup> The mass spectra for each of these samples show the difference in the degree of polymerization range (Figure 1). Inulin P95 has a DP ranging from 3 to 15 with the average DP being 6, while inulin HP has a DP range from 4 to 40 and an average DP of 21.

These average DP measurements were in good agreement with the manufacturer's claim; however, the maximum detectable DP did not strictly agree. The slight disagreement at the upper detectable masses could be due to the differences in the sensitivities of FT-ICR and HPAEC-PAD. FT-ICR is more sensitive in the mass range of 250–5000  $m/z$ , thus a higher DP for inulin P95 is detected. However, the instrument is not optimized for higher  $m/z$  compounds, due to a decrease in ion-transfer efficiency as a result of time-of-flight and ion guide effects, such that a lower DP was detected for inulin HP. These samples further provided a means for improving the high-mass range for the analysis of oligosaccharides with FT-ICR MS. The observation of the inulin peak with a DP 40 at  $m/z$  6523.11 is a new high-mass record for the analysis of oligosaccharides with MALDI FT-ICR MS.

(22) Vorm, O.; Roepstorff, P.; Mann, M. *Anal. Chem.* **1994**, *66*, 3281–3287.

(23) Lastovickova, M.; Chmelik, J. *J. Agric. Food Chem.* **2006**, *54*, 5092–5097.

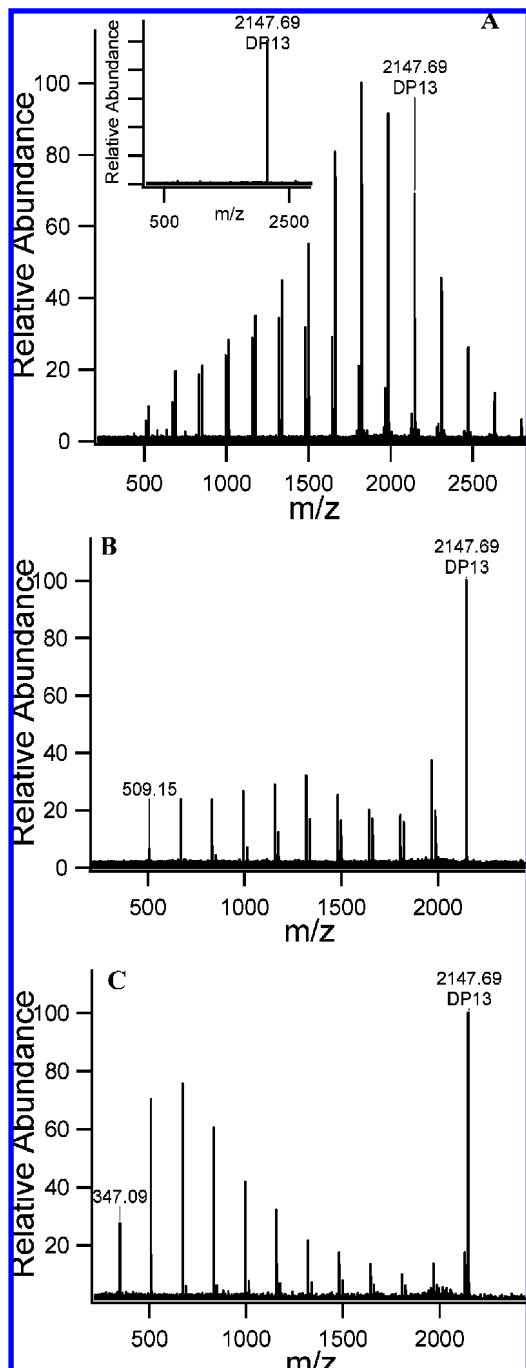


**Figure 2.** MALDI FT-ICR MS positive ion spectra for the elucidation of the structure of inulin HP. (A) Initial mass spectrum before isolation of the DP 13 peak seen in the inset. (B) CID of the DP 13 peak yielded multiple B- and Y-type fragments. (C) IRMPD of the DP 13 peak provided similar fragments as CID; however, it was more efficient in creating smaller fragments.

The major peaks in the mass spectrum for inulin P95 corresponded to the sodium coordinated compounds with a minor series observed at 18 mass units less than the main inulin peaks, perhaps due to in-source decay of higher mass inulin through B-type fragmentation (Figure 1).<sup>24</sup> This fragmentation was differentiated from the possibility of another polymeric series by varying the laser power and observing an increase in fragmenta-

(24) Domon, B.; Costello, C. E. *Glycoconjugate J.* **1988**, *5*, 397–409.

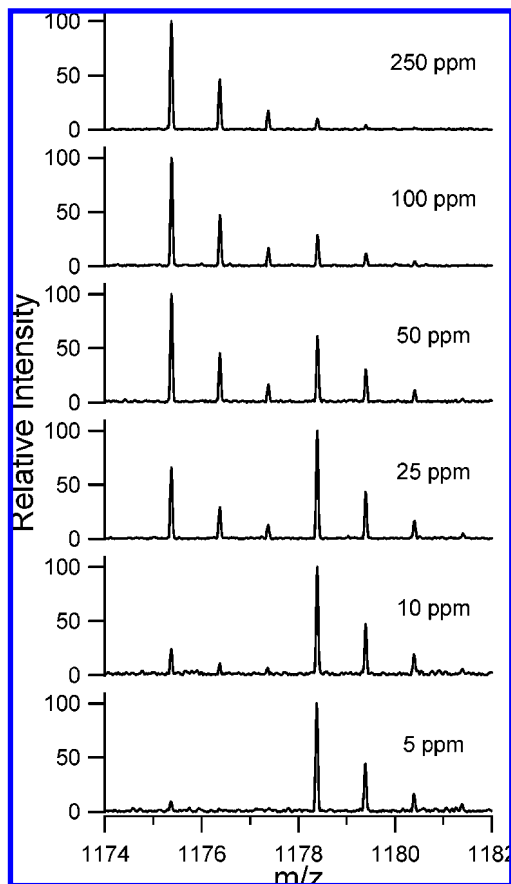


**Figure 3.** MALDI FT-ICR MS positive ion spectra showing the relative abundances of the FOS DP 7 peak and the deuterated reduced maltoheptaose standard. The concentration of the standard was fixed at 1.0  $\mu$ M, and the total FOS concentration was varied. A shift in relative intensity of standard to analyte was observed from 250 to 5 ppm, which was directly correlated to concentration.

tion at higher laser power and a decrease at lower laser power. The inulin HP spectrum was observed to have a higher percentage of these fragment ions, with the fragment ions being more intense than the sodiated molecule up to  $m/z$  3000 as illustrated in the inset. The fragmentation was greater in the case of inulin HP because of the higher DP, which tend to generally produce greater fragmentation. In general, mass analyzers that trap ions produce greater fragmentation during MALDI than those that employ TOF mass analyzers due to the longer time scale of the analysis. To mediate the fragmentation reactions in FT-ICR MS, the instruments are equipped with a high-pressure MALDI source, which allows collisional cooling thereby minimizing fragmentation compared to conventional MALDI FT-ICR MS.<sup>25</sup> The technique of vibrational cooling through collisions was employed in this analysis. Exact mass measurement was used to identify precisely the DP of inulin. With external calibration, the quasimolecular ions were assigned with less than 5 ppm difference between theoretical and calculated mass. The resolution was sufficiently high at the high-mass range (greater than 10 000 full width half-maximum) to verify the assigned DP.

Even with high-mass accuracy and high resolution, tandem mass spectrometry is often required to verify composition and

(25) Zaia, J. *Mass Spectrom. Rev.* **2004**, *23*, 161–227.



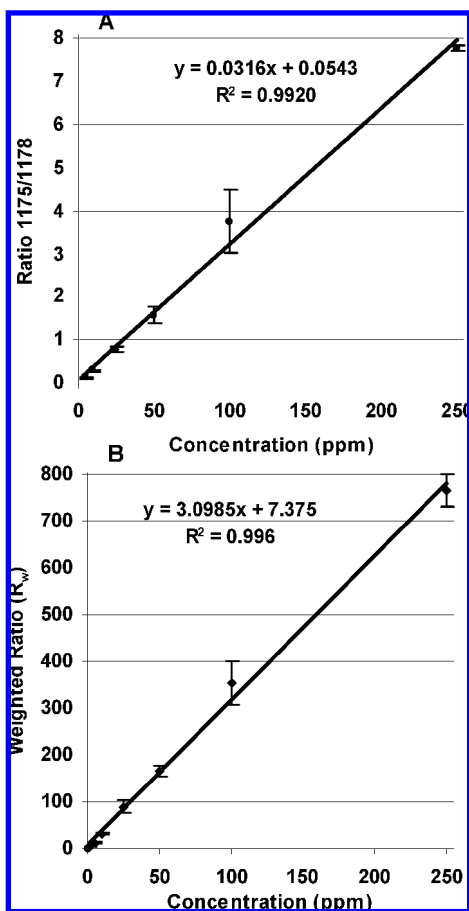


**Figure 4.** Calibration curves for FOS P95. (A) The DP 7 FOS peak to internal standard ratio was plotted versus the concentration of inulin. (B) The weighted ratio versus concentration was plotted. Linear regression was applied to determine the slopes and  $y$  intercepts of the lines of best fit. The error bars indicate the standard deviation of the ratio for the three replicates.

elucidate structures. The inulin HP DP 13 peak (Figure 2A) was isolated and subjected to two complimentary forms of tandem mass spectrometry SORI-CID and IRMPD. The SORI-CID spectrum shows multiple B- and Y-type fragments with the smallest fragment observed at  $509.15 m/z$  corresponding to the  $B_3$  fragment (Figure 2B). The lack of cross-ring cleavages is immediately apparent in the simple spectrum due to the low-energy nature of the CID and the lack of a reducing end, which tends to ring-open and yield cross-ring cleavages. The IRMPD mass spectrum provides additional information yielding fragments that are shifted toward lower masses with the  $B_2$  fragment at  $347.09 m/z$  being the smallest fragment observed (Figure 2C). IRMPD generally yields smaller ions compared to CID, although the degree of fragmentation can be controlled to some extent in both methods. During IRMPD, photon energy is imparted on all ions both precursor and product ions resulting in more extensive fragmentation, while in CID, only the precursor ion is translationally excited and activated. IRMPD is capable of yielding fragments that are typically observed in multiple MS<sup>n</sup> using SORI-CID. Furthermore, we have found IRMPD to be even more efficient for larger oligosaccharides due to an increase in vibration modes with larger compounds, while SORI-CID exhibits a loss in efficiency as molecular weight increases.<sup>14</sup>

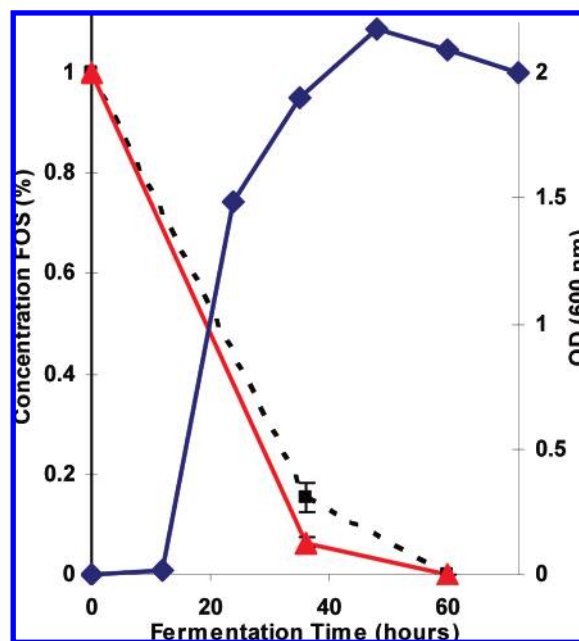


**Figure 5.** Bacterial growth, measured via optical density (OD) at 600 nm of the fermentation, and the concentration of FOS by percent mass plotted versus fermentation time. Squares with dashed line, simple quantitation; triangles with solid line, weighted quantitation, diamonds OD. FOS was the sole carbon source for the fermentation by *B. longum* bv. *infantis*.

**Quantitation of FOS.** With compounds of similar ionization efficiencies, MALDI MS is inherently quantitative within a certain defined mass range.<sup>26–28</sup> For this reason, the total ion abundances are often sufficient for quantitation. For more precise quantitation, an internal standard with similar ionization efficiency when compared to the analyte is necessary. For this purpose, a commercially available maltoheptaose standard was used. The elemental composition and mass of maltose is identical to that of FOS with the same DP; therefore, to differentiate their masses, it was reduced with sodium borodeuteride increasing its mass by three units. In addition, reducing maltose yields an alditol that prohibits cross-ring cleavages at the reducing end and produces a quasimolecular ion that is generally stable with a single peak in the mass spectrum. With the shift in mass, the analyte and the intensities of the internal standard could be measured independently due to the small contribution (5.14%) of the  $M + 3$  isomer peak of the inulin DP 7 to the calibration peak.

To create the calibration curves,  $1.0 \mu\text{M}$  deuterated reduced maltoheptaose was added to the FOS solutions with known concentrations ranging from 500 to 0.1 ppm before spotting on the MALDI plate. The intensity of the internal standard to the analyte peak can be seen to change in a way that is directly proportional to the concentration of FOS in the sample (Figure 3). With the FOS concentration at 250 ppm, the  $m/z$  1175 peak is

(26) Harvey, D. J. *Rapid Commun. Mass Spectrom.* **1993**, *7*, 614–619.

(27) Naven, T. J. P.; Harvey, D. J. *Rapid Commun. Mass Spectrom.* **1996**, *10*, 1361–1366.

(28) Wada, Y.; Azadi, P.; Costello, C. E.; Dell, A.; Dwek, R. A.; Geyer, H.; Geyer, R.; Kakehi, K.; Karlsson, N. G.; Kato, K.; Kawasaki, N.; Khoo, K. H.; Kim, S.; Kondo, A.; Lattova, E.; Mechref, Y.; Miyoshi, E.; Nakamura, K.; Narimatsu, H.; Novotny, M. V.; Packer, N. H.; Perreault, H.; Peter-Katalinic, J.; Pohlentz, G.; Reinhold, V. N.; Rudd, P. M.; Suzuki, A.; Taniguchi, N. *Glycobiology* **2007**, *17*, 411–422.

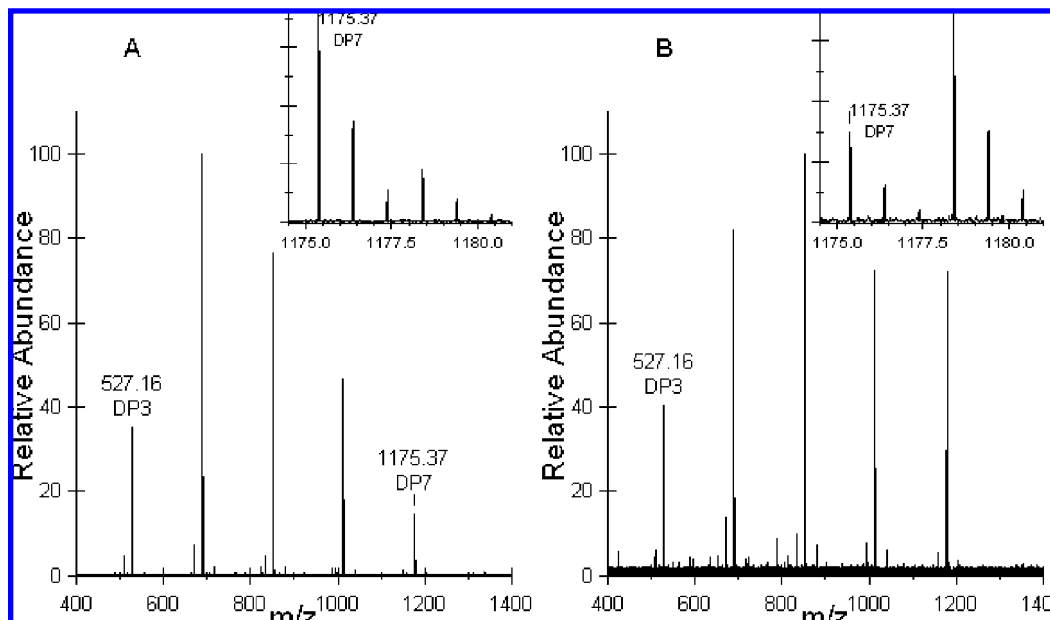


**Figure 6.** MALDI FT-ICR MS positive ion mode spectra of 100 times diluted bacterial fermentation samples of FOS P95 with *B. longum* bv. *infantis*. The inset shows the relative intensities of the internal standard and the FOS DP 7 FOS peak. Fermentation time (A) 0 h; (B) 36 h.

**Table 1. Consumption Data for Each DP FOS at 0, 36, and 60 h Using the Internal Standard**

DP	% consumed		
	0 h	36 h	60 h
3	0	93.0 ± 3.0	100
4	0	95 ± 1.5	100
5	0	91.5 ± 1.5	100
6	0	90.5 ± 1.5	100
7	0	85.5 ± 1.0	100

much more abundant than the  $m/z$  1178 internal standard peak; however, as the FOS concentration is at 5 ppm, it is observed that the internal standard peak is in much greater abundance. In order to obtain more accurate quantitation results, the length of the transient for data processing was decreased to 256k from 1024k data points. Goodner et al. showed that the transient length should be shortened to obtain better ion quantitation due to the dampening of ion signals in FT-ICR MS.<sup>29</sup> After adjustment of the transient length, the absolute intensity of the FOS DP 7 peak was divided by the absolute intensity of the deuterated reduced maltoheptaose standard, in order to obtain an intensity ratio. This intensity ratio was then plotted versus the concentration of the FOS in each sample to obtain a calibration curve (Figure 4A).

The calibration curve based upon a single DP was sufficient for the quantitation of FOS when the individual components of FOS did not vary in intensity. However, due to differential consumption of FOS by the bacteria, another calibration curve was constructed that takes into account each DP of FOS. Equation 1 shows the systematic method of including each DP in a weighted fashion for the quantitation of FOS. The weighting was based upon the fact that the components with higher DP account for a larger amount of average mass than the lower DP ones. The internal standard was still used in order to create a weighted ratio that

was plotted versus concentration (Figure 4B). The efficacy of this method for quantitation of FOS when differential degradation occurs is illustrated later.

Linear regression was then performed on the data sets in order to obtain the lines of best fit; the  $y$  intercept was not fixed to zero so that the limit of detection could be calculated. The linear dynamic range of the calibration was found to be slightly less than 500 ppm of inulin in both cases; however, it does extend to 250 ppm as observed in Figure 4. From 5 to 250 ppm, the calibration curves have excellent linearity with an  $R^2$  value greater than 0.99. The average relative standard deviation for each data point in the calibration curve was less than 8.0% with three replicates for each data point. This deviation can be reduced by acquiring more replicates; nevertheless not much gain is achieved due the high linearity of the existing fit. The LOD was calculated based upon the standard deviation of the  $y$  intercept instead of blank measurements due to the inability to acquire ratios other than zero, a direct result of signal processing. The LOD were calculated to be 8.0 and 5.0 ppm for the simple ratio and the weighted ratio, respectively, with the internal standard at a fixed concentration of 1.0  $\mu\text{M}$ . These values correspond to 7.7 pmol, 4.8 pmol on spot when considering the average DP of FOS to be 6.17, which corresponds to an average molecular mass of 1041 g/mol. The LOD could have been decreased by lowering the concentration of the internal calibrant, to avoid ion suppression; however, FOS is very abundant in real samples such that there is no need to go any lower than 5 ppm, even though the detection limit could be lowered by several orders of magnitude. In addition, the linear dynamic range was the largest when the internal standard was at a concentration of 1.0  $\mu\text{M}$ .

**Bacterial Fermentation of FOS.** Growth of *B. longum* bv. *infantis* was monitored throughout the fermentation of inulin by measuring the  $\text{OD}_{600 \text{ nm}}$  of the culture (Figure 5). In order to perform the quantitation analyses, the samples were diluted such that the observed FOS concentration would fall within the linear

(29) Goodner, K. L.; Milgram, K. E.; Williams, K. R.; Watson, C. H.; Eyley, J. R. *J. Am. Soc. Mass Spectrom.* **1998**, *9*, 1204–1212.

dynamic ranges of the calibration curves. As illustrated in Figure 5, growth of bacteria coincides with consumption of FOS. Using the calibration curves and via addition of the internal standard to the samples, the concentration of FOS after 36 h was determined for each biological replicate with a standard deviation of less than 5%. The simple quantitation using a single DP fell short of accurately quantifying the FOS at 36 h of growth due to differential consumption of the individual components with the lower mass FOS being consumed preferentially first. The concentration of FOS at 36 h was found to be  $630 \pm 25$  ppm using the weighted quantitation method. There was no FOS detected at 60 h, indicating complete consumption by the bacteria.

Figure 6 shows the typical spectra from the fermentation samples with the region of the internal standard inset. It was immediately apparent that the signal-to-noise ratio was much greater at time zero (Figure 6A) than the sample from after 36 h (Figure 6B), indicating a decrease in inulin from 0 to 36 h. It was also apparent in the mass spectra that the relative intensities of each FOS peak change during fermentation with the smaller mass FOS being more abundant before fermentation. In order to observe the differential consumption, the internal standard was used to compare the change in each DP by fermentation (Table 1). The statistically distinct consumption illustrates that there was

preference toward low-mass FOS. The preferential consumption of low-mass FOS by *B. longum* bv. *infantis* is similar to that previously demonstrated by *Bifidobacterium animalis* DN-173 010.<sup>30</sup>

## CONCLUSIONS

Inulin and FOS have been investigated both qualitatively and quantitatively. A method for precise quantitation of FOS was demonstrated, in both a weighted and a simplified fashion via FT-ICR MS. However, the method is readily transportable to other MS techniques. The utility of the weighted method has been illustrated by quantifying FOS at different time points during bacterial fermentation. The simplified method can be applied to the quantitation of FOS and inulin in foods and plants, thus enhancing the researcher's ability to rapidly and precisely investigate these oligosaccharides, or any other polymeric system.

## ACKNOWLEDGMENT

Financial support was provided by the California Dairy Research Foundation, Dairy Management Incorporated, the National Institutes of Health, and the University of California Discovery Grant (05GEB01NHB).

Received for review August 15, 2007. Accepted October 11, 2007.

AC7017298

(30) Van der Meulen, R.; Avonts, L.; De Vuyst, L. *Appl. Environ. Microbiol.* **2004**, *70*, 1923–1930.